Computer Assisted Proofs of Fiberwise Hyperbolic Invariant Tori in skew-products over rotations.

Jordi-Lluís Figueras[1]

[1]Matematiska Institutionen
Uppsala University

20141113

GOALS:

1. How to implement Computer Assisted Proofs of FHIT.
2. Show that CAPs of FHIT can be performed in an accurate manner.

We will see that with the help of Analysis CAPs can be performed with very accurate results.

We will see that with the help of Analysis CAPs can be performed with very accurate results.

But not everyone agree...

We will see that with the help of Analysis CAPs can be performed with very accurate results.

But not everyone agree...

I was once visiting Krakow and said:

We will see that with the help of Analysis CAPs can be performed with very accurate results.

But not everyone agree...

I was once visiting Krakow and said:

> *" Analytical tools can produce finer results than topological methods."*
>
> *Anonymous*

We will see that with the help of Analysis CAPs can be performed with very accurate results.

But not everyone agree...

I was once visiting Krakow and said:

> *" Analytical tools can produce finer results than topological methods."*
>
> *Anonymous*

And someone in the audience replied:

We will see that with the help of Analysis CAPs can be performed with very accurate results.

But not everyone agree...

I was once visiting Krakow and said:

> *" Analytical tools can produce finer results than topological methods."*
>
> *Anonymous*

And someone in the audience replied:

> *" And tell me, friend, when did Saruman the Wise abandon reason for madness?"*
>
> *Gandalf the Gray.*

We will see that our results can be only improved with technology, but not with mathematics.

Outline of topics

Set up.

FHIT in skew-products.

A **skew-product** over a rotation is a smooth map of the form

$$\begin{array}{ccc} \mathbb{R}^n \times \mathbb{T}^d & \longrightarrow & \mathbb{R}^n \times \mathbb{T}^d \\ \begin{pmatrix} z \\ \theta \end{pmatrix} & \longrightarrow & \begin{pmatrix} F(z,\theta) \\ \theta + \omega \end{pmatrix} \end{array},$$

where ω is the rotation vector.

FHIT. Dynamical definition.

A **FHIT** is a graph of a continuous map $K\colon \mathbb{T}^d \to \mathbb{R}^n$ such that:

1. **Invariance:** $K(\theta + \omega) = F(K(\theta), \theta), \quad \forall \theta \in \mathbb{T}^d.$
2. **Hyperbolicity:** The fiber bundle $\mathbb{R}^n \times \mathbb{T}^d$ decomposes in a continuous invariant Whitney sum $E^s \oplus E^u$ such that $D_z F_{|E^u}$ is invertible and there exist $0 < \lambda < 1$ and $C > 0$ for which
   - If $(v, \theta) \in E^s$ and $m > 0$, then
   $$||D_z F^m(K(\theta), \theta)v|| < C\lambda^m ||v||.$$
   - If $(v, \theta) \in E^u$ and $m < 0$, then
   $$||D_z F^m(K(\theta), \theta)v|| < C\lambda^{-m} ||v||.$$

FHIT. Functional definition.

A **FHIT** is a graph of a continuous map $K \colon \mathbb{T}^d \to \mathbb{R}^n$ such that:

1. **Invariance:** K is a zero of

$$\begin{array}{rccc} \mathcal{F}\colon & \mathcal{C}(\mathbb{T}^d, \mathbb{R}^n) & \longrightarrow & \mathcal{C}(\mathbb{T}^d, \mathbb{R}^n) \\ & K & \longrightarrow & F(K(\theta - \omega), \theta - \omega) - K(\theta) \end{array} .$$

2. **Hyperbolicity:** The transfer operator

$$\begin{array}{rccc} D\mathcal{F}\colon & \mathcal{C}(\mathbb{T}^d, \mathbb{R}^n) & \longrightarrow & \mathcal{C}(\mathbb{T}^d, \mathbb{R}^n) \\ & \sigma & \longrightarrow & D_z F(K(\theta - \omega), \theta - \omega)\sigma(\theta - \omega) \end{array} .$$

is hyperbolic, i.e. the unit circle is contained in its resolvent.

Validation algorithm.

Validation algorithm.

We use algorithms based on an adaptation of the Newton-Kantorovich theorem to the problem. See

A. Haro and R. de la Llave.
A parameterization method for the computation of invariant tori and their whiskers in quasi periodic maps: numerical algorithms.
Discrete and Continuous Dynamical Systems. Serie B 6-(6): 1261-1300, 2006.

The core: Newton-Kantorovich theorem.

Theorem's: Let $\mathcal{F}\colon \Omega \subset B \to B$ be a $\mathcal{C}^2$ operator on a Banach space. Let $B(x_0, r) \subset \Omega$. Suppose that:

- $D\mathcal{F}(x_0)$ has a continuous inverse.
- $||D\mathcal{F}^{-1}(x_0) \cdot \mathcal{F}(x_0)|| \leq \varepsilon$.
- $||D\mathcal{F}^{-1}(x_0) \cdot D^2\mathcal{F}(x)|| \leq \beta$, for $x \in B(x_0, r)$.

Suppose also that

$$h = \varepsilon\beta \leq \frac{1}{2},$$

and define the constants

$$r_0 = \frac{1 - \sqrt{1 - 2h}}{h}\varepsilon, \quad r_1 = \frac{1 + \sqrt{1 - 2h}}{h}\varepsilon.$$

Then, if $r_0 < r < r_1$ the map $\mathcal{F}$ has a zero in the ball $B(x_0, r_0)$ and it is unique in the ball $B(x_0, r)$.

Validation algorithm. Step 0 of 5.

0.1.- Compute the initial data:
Ask Àlex Haro!

Validation algorithm. Step 0 of 5.

0.1.- Compute the initial data:
Ask Àlex Haro!

- An approximate invariant torus $K\colon \mathbb{T}^d \to \mathbb{R}^n$.
- Two continuous matrix-valued maps $P_1, P_2\colon \mathbb{T}^d \to GL(n, \mathbb{R})$, where P_1 has in its columns an approximation of the invariant subbundles and P_2 is an approximate inverse of P_1.
- A continuous block diagonal matrix-valued map $\Lambda\colon \mathbb{T}^d \to GL(n, \mathbb{R})$ which satisfies, approximately

$$P_2(\theta + \omega) D_z F(K(\theta), \theta) P_1(\theta) \simeq \Lambda(\theta) = \begin{pmatrix} \Lambda_{n_s}(\theta) & 0 \\ 0 & \Lambda_{n_u}(\theta) \end{pmatrix}.$$

Λ modelizes approximately the dynamics on the invariant subbundles.

Validation algorithm. Step 1 of 5.

1.1.- Compute the upper bounds:

- $$||P_2(\theta+\omega)D_zF(K(\theta),\theta)P_1(\theta)-\Lambda(\theta)||_\infty \le \sigma$$

- $$||P_2(\theta)P_1(\theta)-\mathrm{Id}||_\infty \le \tau$$

- $$\max\left\{||\Lambda_{n_s}(\theta)||_\infty, ||\Lambda_{n_u}(\theta)^{-1}||_\infty\right\} \le \lambda$$

1.2.- Check $\lambda+\sigma+\tau<1$. If not, validation fails.

Validation algorithm. Step 2 of 5.

2.1.- Compute the upper bound:

$$||P_2(\theta)\,(F(K(\theta-\omega),\theta-\omega)-K(\theta))\,||_\infty \leq \rho$$

2.2.- Compute the upper bound:

$$\frac{\rho}{1-(\lambda+\sigma+\tau)} \leq \varepsilon.$$

Validation algorithm. Step 3 of 5.

3.1.- Compute the upper bound:

$$\left|\left|P_2(\theta+\omega)D_z^2F(z(\theta),\theta)\left[P_1(\theta)\cdot,P_1(\theta)\cdot\right]\right|\right|_\infty \leq b$$

for $z(\theta) \in B(K(\theta), 2(1+\tau)\varepsilon)$.

3.2.- Compute the uppers bounds:

$$\frac{b}{1-(\lambda+\sigma+\tau)} \leq \beta, \quad \beta\varepsilon \leq h.$$

Validation algorithm. Step 4 of 5.

4.1.- If $h < \frac{1}{2}$ there exists an invariant torus $K_* : \mathbb{T} \to \mathbb{R}^n$ with

$$||P_1(\theta)^{-1}(K_*(\theta) - K(\theta))||_\infty < r_0$$

where

$$\frac{1 - \sqrt{1 - 2h}}{h} \cdot \varepsilon \leq r_0.$$

Moreover, this invariant torus is unique in the ball centered at the approximate invariant torus K_0 and radius

$$r_1 \leq \frac{1 + \sqrt{1 - 2h}}{h} \cdot \varepsilon.$$

Validation algorithm. Step 5 of 5.

5.1.- Compute the upper bounds:

- $||\Lambda(\theta)||_\infty \le \hat{\lambda}$.
-
$$\frac{\lambda}{1-\lambda^2}\frac{1}{1-\tau}\left(br_0+\sigma+\hat{\lambda}\tau\right) \le \mu.$$

5.2.- If $\mu < \frac{1}{4}$ then:

- The distance between the bundles is smaller than
$$\frac{\mu}{\sqrt{1-4\mu}}.$$
-
$$||\Lambda_*(\theta)-\Lambda(\theta)||_\infty \le \frac{1}{1-\tau}\left(br_0+\sigma+\hat{\lambda}\tau\right)\left(1+\frac{\mu}{\sqrt{1-4\mu}}\right),$$

Validation procedure.

The validation procedure is:

1. Obtain initial data via some (non-rigorous) numerical method.
2. Transform initial data to Fourier model.
3. Perform the validation algorithm with the Fourier model data.

Fourier models.

Fourier models.

There are several ways we can rigorously represent on a computer periodic functions:

- Interpolation polynomials.
- Cubic splines.
- Piece-wise Taylor models.
- Fourier polynomials.
- ...

Fourier models.

We have chosen **Fourier polynomials** because they are the most suitable in the context of skew-products over rotations.

Important property: The operator $S_\omega \colon L^2(\mathbb{T},\mathbb{R}) \to L^2(\mathbb{T},\mathbb{R})$, $(S_\omega f)(\theta) = f(\theta+\omega)$ *diagonalizes.* That is,

$$e^{2\pi k i\theta} \to e^{2\pi i k\omega} e^{2\pi k i\theta}$$

Fourier models.

Definition: A **(real) Fourier model** of order N consists of two sequences of real intervals $\{a_k\}_{k=0}^N$, $\{b_k\}_{k=1}^N$ and an additional real interval $\mathcal{R}$.
We will say that a continous function $f : \mathbb{T} \to \mathbb{R}$ is enclosed by the Fourier model if, $\forall \theta \in \mathbb{T}$

$$f(\theta) \in a_0 + \sum_{k=1}^{N} a_k \cos(2\pi k\theta) + \sum_{k=1}^{N} b_k \sin(2\pi k\theta) + \mathcal{R}.$$

Remark: The interval $\mathcal{R}$ is used to check the growth of error on the operations.

Fourier models' computations.

Let F and G be two N-order Fourier models and let J be any interval.

For our purposes we have implemented, in **C++**, the following operations between Fourier models:

Fourier models' computations.

Let F and G be two N-order Fourier models and let J be any interval.

For our purposes we have implemented, in **C++**, the following operations between Fourier models:

- Evaluation $F(J)$.
- $||F||_\infty$.
- $F \pm G$, $J \cdot G$.
- Translation $F(\theta + J)$.
- $F \cdot G$.
- $\sin(F)$, $\cos(F)$.

Example 1.

Quasiperiodic standard map.

The **quasiperiodic standard map** is defined as the skew-product

$$\begin{cases} \bar{x} &=& x + \bar{y} \\ \bar{y} &=& y - \frac{\kappa}{2\pi}\sin(2\pi x) - \varepsilon \sin(2\pi\theta) \\ \bar{\theta} &=& \theta + \omega \pmod 1 \end{cases} .$$

We fix $\kappa > 0$ and ω the golden mean.

Quasiperiodic standard map.

When $\varepsilon = 0$ and $\kappa > 0$ the dynamics on the fiber is uncoupled from the torus. The system has the FHIT

$$\left\{ \left(\frac{1}{2}, 0, \theta \right) \mid \theta \in \mathbb{T} \right\}.$$

We have continued numerically the torus through ε and computed its maximal Lyapunov multiplier and the distance between its invariant subbundles.

Numerical exploration $\kappa = 1.3$.

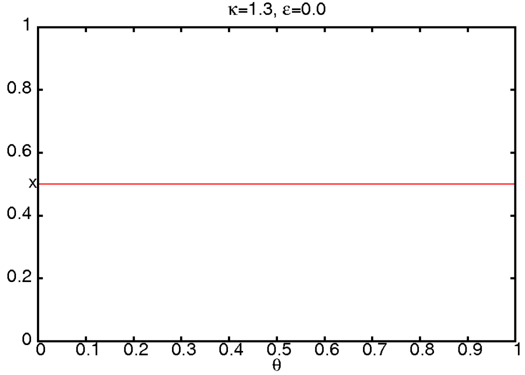

Figure: x-projection invariant torus. $\kappa = 1.3$, $\varepsilon = 0.0$.

Numerical exploration $\kappa = 1.3$.

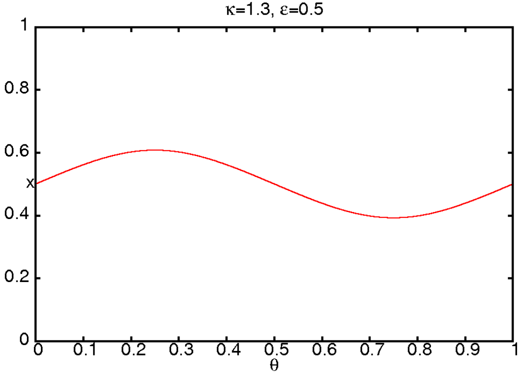

Figure: x-projection invariant torus. $\kappa = 1.3$, $\varepsilon = 0.5$.

Numerical exploration $\kappa = 1.3$.

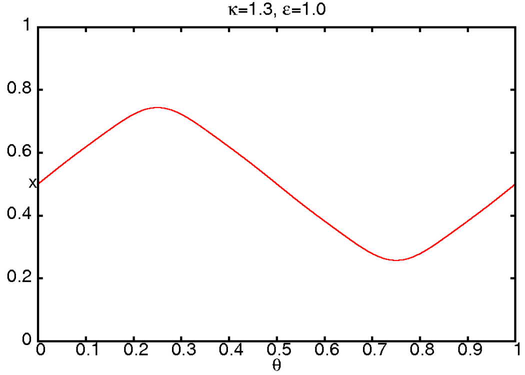

Figure: x-projection invariant torus. $\kappa = 1.3$, $\varepsilon = 1.0$.

Numerical exploration $\kappa = 1.3$.

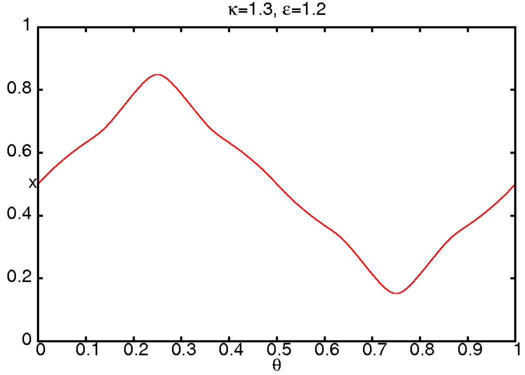

Figure: x-projection invariant torus. $\kappa = 1.3$, $\varepsilon = 1.2$.

Numerical exploration $\kappa = 1.3$.

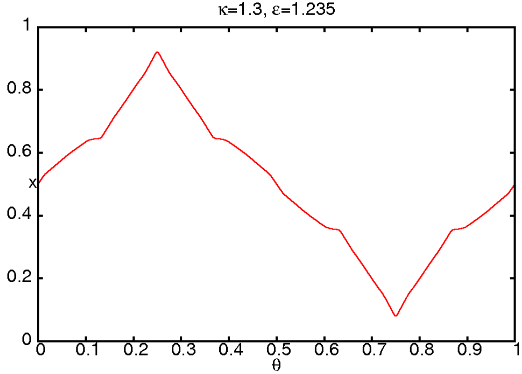

Figure: x-projection invariant torus. $\kappa = 1.3$, $\varepsilon = 1.235$.

Numerical exploration $\kappa = 1.3$.

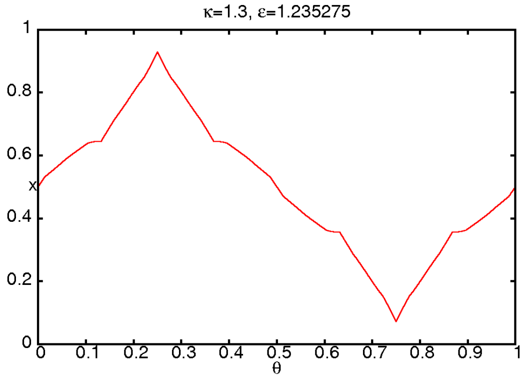

Figure: x-projection invariant torus. $\kappa = 1.3$, $\varepsilon = 1.235275$.

Numerical exploration $\kappa = 1.3$.

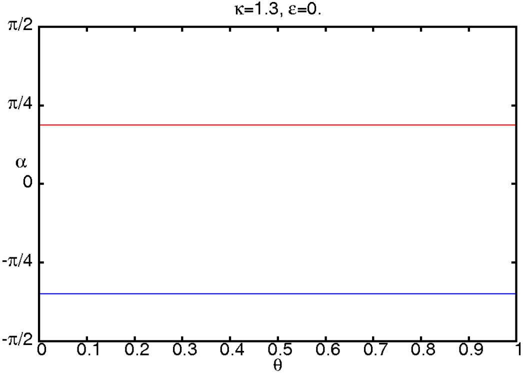

Figure: Invariant bundles. $\kappa = 1.3$, $\varepsilon = 0.0$.

Numerical exploration $\kappa = 1.3$.

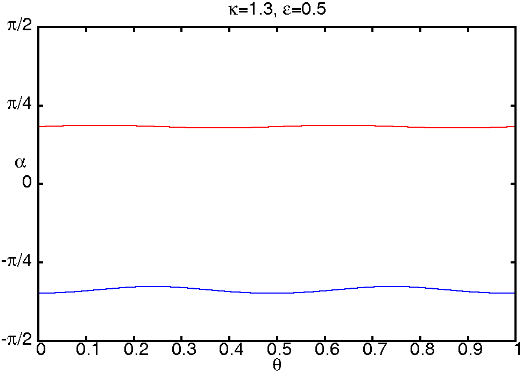

Figure: Invariant bundles. $\kappa = 1.3$, $\varepsilon = 0.5$.

Numerical exploration $\kappa = 1.3$.

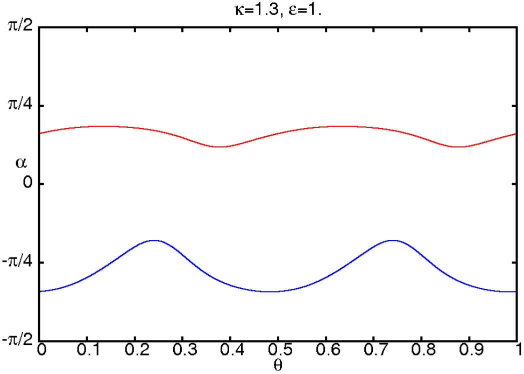

Figure: Invariant bundles. $\kappa = 1.3$, $\varepsilon = 1.0$.

Numerical exploration $\kappa = 1.3$.

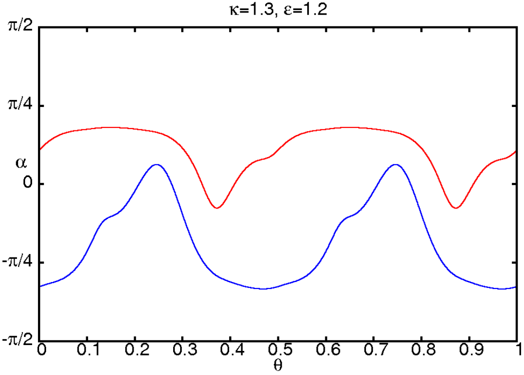

Figure: Invariant bundles. $\kappa = 1.3$, $\varepsilon = 1.2$.

Numerical exploration $\kappa = 1.3$.

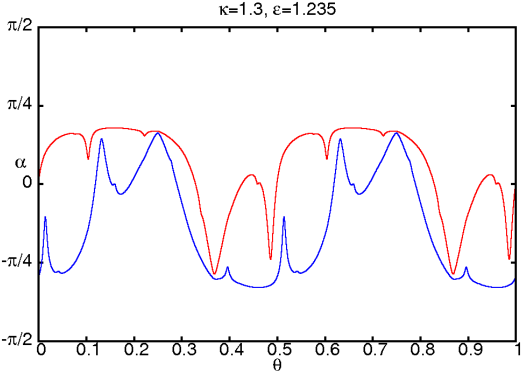

Figure: Invariant bundles. $\kappa = 1.3$, $\varepsilon = 1.235$.

Numerical exploration $\kappa = 1.3$.

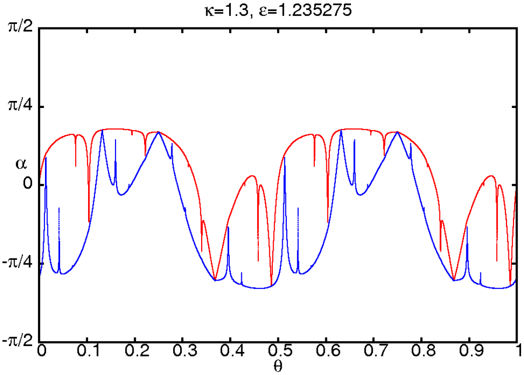

Figure: Invariant bundles. $\kappa = 1.3$, $\varepsilon = 1.235275$.

Numerical exploration $\kappa = 1.3$.

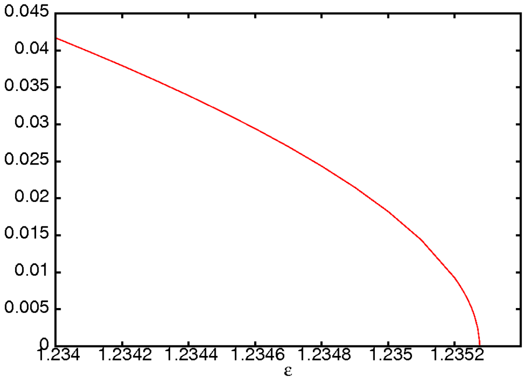

Figure: Distance between subbundles for $\kappa = 1.3$.

Numerical exploration $\kappa = 1.3$.

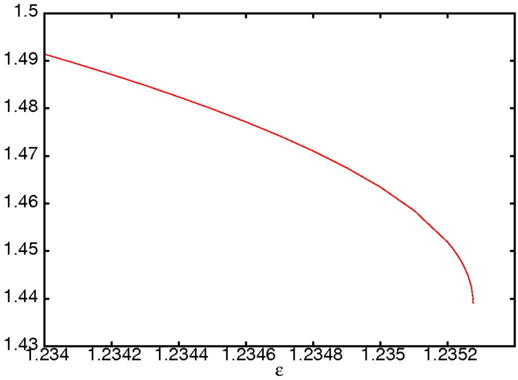

Figure: Lyapunov multiplier for $\kappa = 1.3$.

Numerical exploration $\kappa = 1.3$.

Numerator	Denominator	ε_c	Λ_c
610	987	1.235277250097	1.417569758833
987	1597	1.235276717863	1.427183182503
⋮	⋮	⋮	⋮
514229	832040	1.235275526885	1.439118021353
832040	1346269	1.235275526763	1.439124814800
1346269	2178309	1.235275526763	1.439124666214
2178309	3524578	1.235275526763	1.439124723263
3524578	5702887	1.235275526763	1.439124701574

Table: Critical ε_c where the transition occur and their Lyapunov multiplier Λ_c for each of the partial convergents of the golden mean with denominator less than $6 \cdot 10^6$. $\kappa = 1.3$.

By the above table we obtain that the breakdown value, ε_c, is near

$$1.235275526763.$$

Validation results for $\kappa = 1.3$.

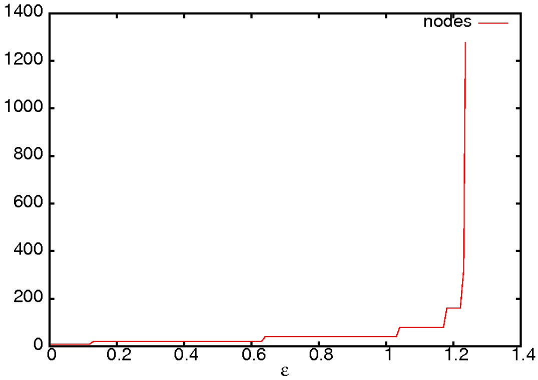

Figure: Number of nodes used on the validation.

Validation results for $\kappa = 1.3$.

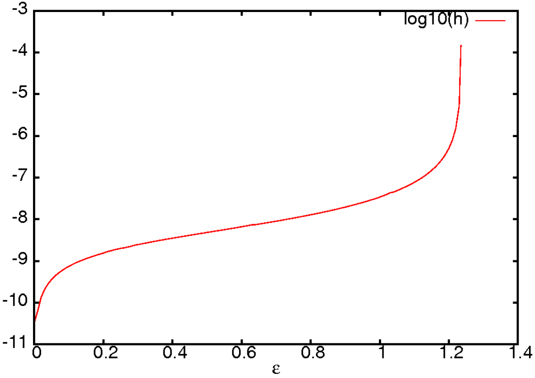

Figure: *h* value of the validation.

Validation results for $\kappa = 1.3$.

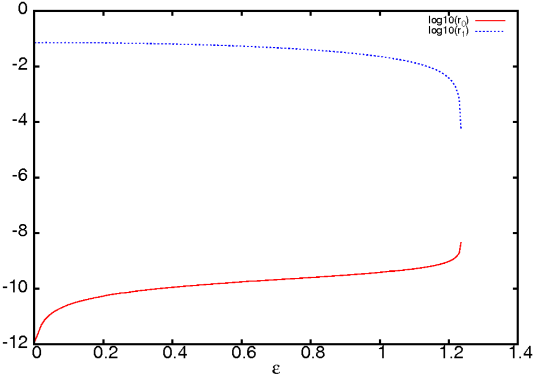

Figure: r_0 and r_1 values of the validation.

Validation results for $\kappa = 1.3$.

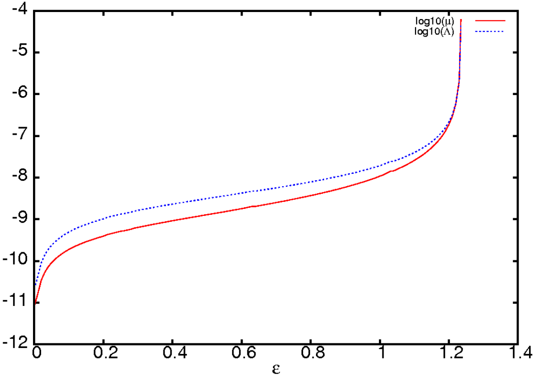

Figure: Observables distance values of the validation.

Validation results for $\kappa = 1.3$, near breakdown.

We have validated the existence of FHIT until $\varepsilon = 1.235275$.

The maximum difference between the biggest predicted breakdown value and the last validation is less than

$$5.27 \cdot 10^{-7}$$

ϵ	h	r_0	r_1	Number of nodes	comp. time(min)
1.235270	$2.853269e-03$	$1.302039e-07$	$9.100589e-05$	5802	100
1.235273	$8.140590e-03$	$2.490723e-07$	$6.069352e-05$	7918	153
1.235275	$8.928078e-02$	$1.035418e-06$	$2.107294e-05$	27692	1094

Table: Validation results near the breakdown predicted value $\varepsilon_c \simeq 1.235275526763$

The growth of the number of nodes is due to the wildness of the invariant bundles!

Number of nodes vs Time computation.

Number of nodes	comp. time(min)
40	0.458167
540	6.446334
1040	12.74084
1540	19.63984
2040	27.17817
2540	35.02600
3040	44.29384
3540	52.66734
4040	61.95984
4540	71.92917
5040	82.33534
5540	93.29884

Table: Validation time cost depends on the number of nodes.

Example 2.

Driven logistic map.

The **driven logistic map** is defined as the skew-product

$$
\begin{array}{rccc}
f: & \mathbb{R}\times\mathbb{T} & \longrightarrow & \mathbb{R}\times\mathbb{T} \\
 & (z,\theta) & \longrightarrow & (a(1+D\cos(2\pi\theta))z(1-z),\theta+\omega)
\end{array},
$$

where $\omega = \frac{\sqrt{5}-1}{2}$; and a and D are parameters. Along this example we will fix $D = 0.1$ and let a vary.

Numerical exploration. $D = 0.1$.

Numerical facts:

- It has a repellor curve for all $a > 3.143$.

Numerical exploration. $D = 0.1$.

Numerical facts:

- It has a repellor curve for all $a > 3.143$.
- It has a 2 period attracting curve for $3.143 < a < 3.271383$.

Numerical exploration. $D = 0.1$.

Numerical facts:

- It has a repellor curve for all $a > 3.143$.
- It has a 2 period attracting curve for $3.143 < a < 3.271383$.
- For $3.143 < a < 3.17496$ the attracting curve is reductible.

Numerical exploration. $D = 0.1$.

Numerical facts:

- It has a repellor curve for all $a > 3.143$.
- It has a 2 period attracting curve for $3.143 < a < 3.271383$.
- For $3.143 < a < 3.17496$ the attracting curve is reductible.
- For $3.17496 < a < 3.271383$ the attracting curve is **NOT** reductible, that is, is non-invertible.

Numerical exploration. $D = 0.1$.

Numerical facts:

- It has a repellor curve for all $a > 3.143$.
- It has a 2 period attracting curve for $3.143 < a < 3.271383$.
- For $3.143 < a < 3.17496$ the attracting curve is reductible.
- For $3.17496 < a < 3.271383$ the attracting curve is **NOT** reductible, that is, is non-invertible.
- Aparently, at $a \simeq 3.271383$ the attracting curve suffers a non-smooth bifurcation to a SNA.

Numerical exploration. $D = 0.1$.

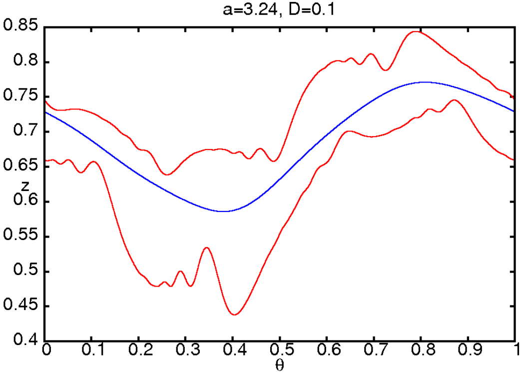

Figure: 2-period attracting curve for $a = 3.24$.

Numerical exploration. $D = 0.1$.

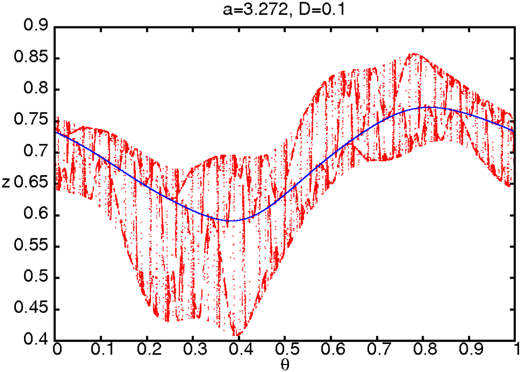

Figure: 2-period attracting curve for $a = 3.272$.

Numerical exploration. $D = 0.1$.

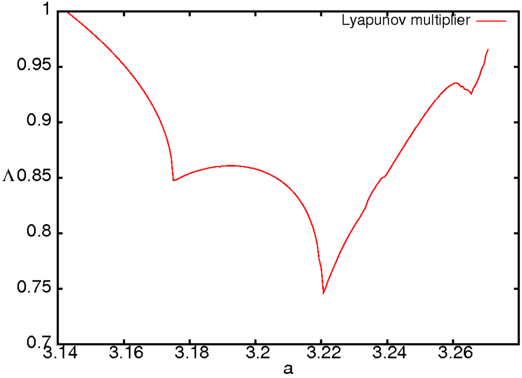

Figure: Lyapunov multiplier of the 2-periodic attracting curve.

Validation results.

In order to validate the 2 period invariant torus, we use the composition map and apply the validation algorithm explained before.
The composition map is

$$\begin{array}{rccc} F: & \mathbb{R}\times\mathbb{T} & \longrightarrow & \mathbb{R}\times\mathbb{T} \\ & (z,\theta) & \longrightarrow & (f(f(z,\theta),\theta+\omega),\theta+2\omega) \end{array}.$$

Validation results.

We have validated the 2 period attracting curve for several values of $a \in [3.143, 3.265]$, in particular, for $a = 3.26$ and $a = 3.265$. (In this values it is **not reductible**).
Due to the non reductible nature, the slopes of some initial data are quite high. For example, at $a = 3.265$, the maximum slope of P_1 is $4.3 \cdot 10^4$, and the maximum slope of the torus is $3 \cdot 10^3$.

Maximum slopes data.

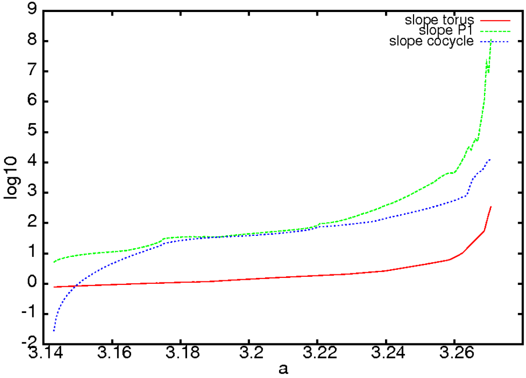

Figure: Maximum slopes of initial data depending on a.

Validated torus $a = 3.26$.

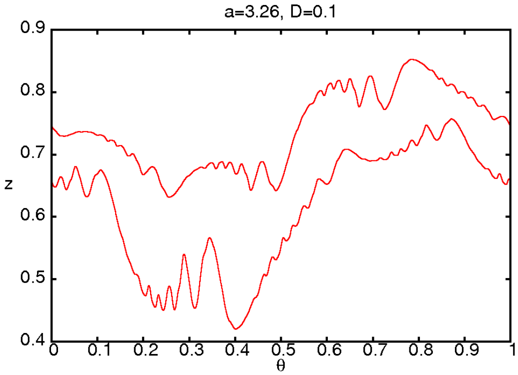

Figure: 2 period attracting torus for $a = 3.26$.

Validated torus $a = 3.265$.

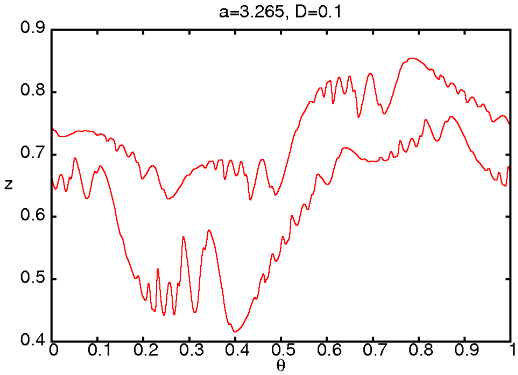

Figure: 2 period attracting torus for $a = 3.265$.

Validated torus $a = 3.26$.

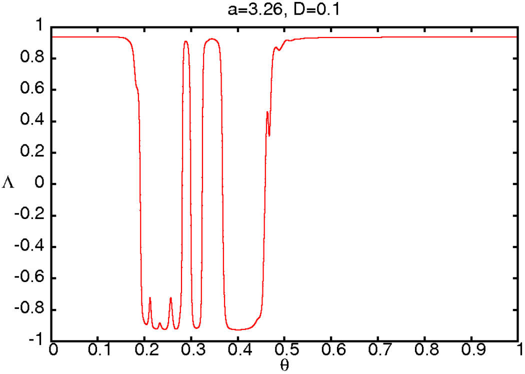

Figure: Λ "matrix" for $a = 3.26$.

Validated torus $a = 3.265$.

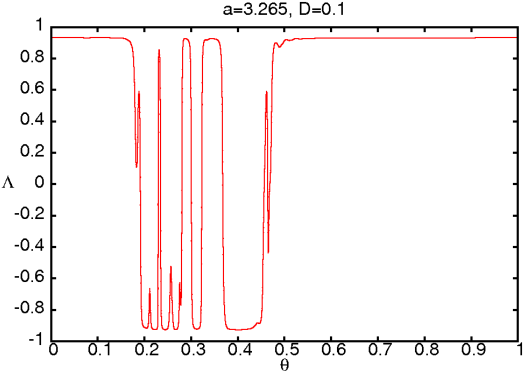

Figure: Λ "matrix" for $a = 3.265$.

Validated torus $a = 3.26$.

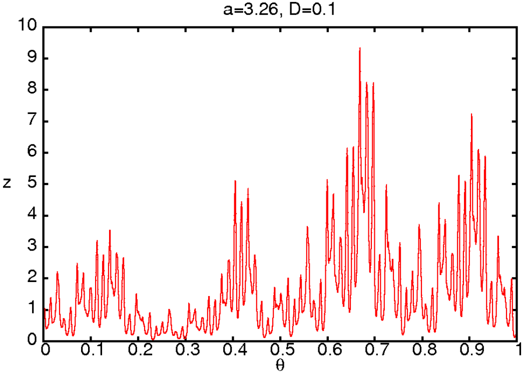

Figure: $P1$ change of variables for $a = 3.26$.

Validated torus $a = 3.265$.

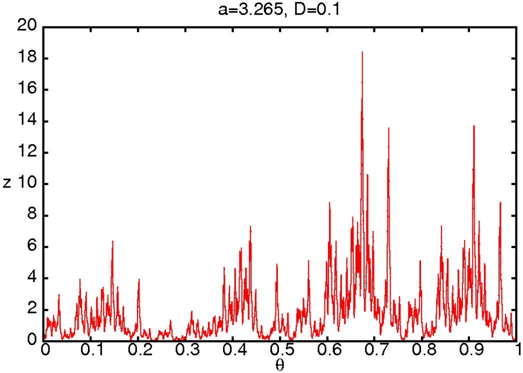

Figure: $P1$ change of variables for $a = 3.265$.

Validation results.

a	3.26	3.265
Number of nodes	2000	5000
h	1.055098e-05	4.684567e-05
r_0	3.637170e-08	7.542679e-08
r_1	6.894395e-03	3.220074e-03
$\|\|\Lambda\|\|_\infty$	9.428802e-01	9.466133e-01
$\|\|\Lambda_* - \Lambda\|\|_\infty$	5.764746e-06	2.255056e-05

Table: Validation results of the period 2 invariant torus of the driven logistic map with $a = 3.26$ and $a = 3.265$.

These validations are very easy to carry on with the methodology presented here.
Topological methods (Krakow) have not succeded in proving these tori.

Conclusions and final words

Conclusions and final words:

- We apply the validation algorithm in two challenging problems.
- The limitations of the algorithm are the wildness of the initial data we want to validate.
- We have also implement the validation of families of FHIT.

Thank you very much!

Jordi-Lluís Figueras
Uppsala University
figueras@math.uu.se